

SCORING AND CLASSIFYING WITH GATED AUTO-ENCODERS

Daniel Jiwoong Im & Graham W. Taylor

School of Engineering
University of Guelph
Guelph, Ontario, Canada N1G2W1
{imj, gwtaylor}@uoguelph.ca

ABSTRACT

Auto-encoders are perhaps the best-known non-probabilistic methods for representation learning. They are conceptually simple and easy to train. Recent theoretical work has shed light on their ability to capture manifold structure, and drawn connections to density modeling. This has motivated researchers to seek ways of auto-encoder scoring, which has furthered their use in classification. Gated auto-encoders (GAEs) are an interesting and flexible extension of auto-encoders which can learn transformations among different images or pixel covariances within images. However, they have been much less studied, theoretically or empirically. In this work, we apply a dynamical systems view to GAEs, deriving a scoring function, and drawing connections to RBMs. On a set of deep learning benchmarks, we also demonstrate their effectiveness for single and multi-label classification.

1 INTRODUCTION

Representation learning algorithms are machine learning algorithms which involve the learning of features or explanatory factors. Deep learning techniques, which employ several layers of representation learning, have achieved much recent success in machine learning benchmarks and competitions, however, most of these successes have been achieved with purely supervised learning methods and have relied on large amounts of labeled data (Krizhevsky et al., 2012; Szegedy et al., 2014). Though progress has been slower, it is likely that unsupervised learning will be important to future advances in deep learning (Bengio & Thibodeau-Laufer, 2013).

The most successful and well-known example of non-probabilistic unsupervised learning is the auto-encoder. Conceptually simple and easy to train via backpropagation, various regularized variants of the model have recently been proposed (Rifai, 2011; Vincent et al., 2008; Swersky et al., 2011) as well as theoretical insights into their operation (Vincent, 2010; Guillaume & Bengio, 2013).

In practice, the latent representation learned by auto-encoders has typically been used to solve a secondary problem, often classification. The most common setup is to train a single auto-encoder on data from all classes and then a classifier is tasked to discriminate among classes. However, this contrasts with the way probabilistic models have typically been used in the past: in that literature, it is more common to train one model per class and use Bayes’ rule for classification. There are two challenges to classifying using per-class auto-encoders. First, up until very recently, it was not known how to obtain the score of data under an auto-encoder, meaning how much the model “likes” an input. Second, auto-encoders are non-probabilistic, so even if they can be scored, the scores do not integrate to 1 and therefore the per-class models need to be calibrated.

Kamyshanska & Memisevic (2013) have recently shown how scores can be computed from an auto-encoder by interpreting it as a dynamical system. Although the scores do not integrate to 1, they show how one can combine the unnormalized scores into a generative classifier by learning class-specific normalizing constants from labeled data.

In this paper we turn our interest towards a variant of auto-encoders which are capable of learning higher-order features from data (Memisevic, 2011). The main idea is to learn relations between pixel intensities rather than the pixel intensities themselves by structuring the model as a tri-partite graph which connects hidden units to pairs of images. If the images are different, the hidden units learn how the images transform. If the images are the same, the hidden units encode within-image

pixel covariances. Learning such higher-order features can yield improved results on recognition and generative tasks.

We adopt a dynamical systems view of gated auto-encoders, demonstrating that they can be scored similarly to the classical auto-encoder. We develop a theory which yields insights into the operation of gated auto-encoders. In addition to the theory, we show in our experiments that a classification model based on gated auto-encoder scoring can outperform a number of other representation learning architectures, including classical auto-encoder scoring. We also demonstrate that scoring can be useful for the structured output task of multi-label classification.

2 GATED AUTO-ENCODERS

In this section, we review the gated auto-encoder (GAE). Due to space constraints, we will not review the classical auto-encoder. Instead, we direct the reader to the reviews in (Memisevic, 2011; Kamyshanska & Memisevic, 2013) with which we share notation. Similar to the classical auto-encoder, the GAE consists of an encoder $h(\cdot)$ and decoder $r(\cdot)$. While the standard auto-encoder processes a datapoint \mathbf{x} , the GAE processes input-output pairs (\mathbf{x}, \mathbf{y}) . The GAE is usually trained to reconstruct \mathbf{y} given \mathbf{x} , though it can also be trained symmetrically, that is, to reconstruct both \mathbf{y} from \mathbf{x} and \mathbf{x} from \mathbf{y} . Intuitively, the GAE learns *relations* between the inputs, rather than representations of the inputs themselves¹. If $\mathbf{x} \neq \mathbf{y}$, for example, they represent sequential frames of a video, intuitively, the mapping units \mathbf{h} learn *transformations*. In the case that $\mathbf{x} = \mathbf{y}$ (i.e. the input is copied), the mapping units learn pixel covariances.

In the simplest form of the GAE, the M hidden (mapping) units are given by a basis expansion of \mathbf{x} and \mathbf{y} . However, this leads to a parameterization that it is at least quadratic in the number of inputs and thus, prohibitively large. Therefore, in practice, \mathbf{x} , \mathbf{y} , and \mathbf{h} are projected onto matrices or (“latent factors”), W^X , W^Y , and W^H , respectively. The number of factors, F , must be the same for X , Y , and H . Thus, the model is completely parameterized by $\theta = \{W^X, W^Y, W^H\}$ such that W^X and W^Y are $F \times D$ matrices (assuming both \mathbf{x} and \mathbf{y} are D -dimensional) and W^H is an $M \times F$ matrix. The encoder function is defined by

$$h(\mathbf{x}, \mathbf{y}) = \sigma(W^H((W^X \mathbf{x}) \odot (W^Y \mathbf{y}))) \quad (1)$$

where \odot is element-wise multiplication and $\sigma(\cdot)$ is an activation function. The decoder function is defined by

$$r(\mathbf{y}|\mathbf{x}, h) = (W^Y)^T((W^X \mathbf{x}) \odot (W^H)^T h(\mathbf{x}, \mathbf{y})). \quad (2)$$

$$r(\mathbf{x}|\mathbf{y}, h) = (W^X)^T((W^Y \mathbf{y}) \odot (W^H)^T h(\mathbf{x}, \mathbf{y})), \quad (3)$$

Note that the parameters are usually shared between the encoder and decoder. The choice of whether to apply a nonlinearity to the output, and the specific form of objective function will depend on the nature of the inputs, for example, binary, categorical, or real-valued. Here, we have assumed real-valued inputs for simplicity of presentation, therefore, Eqs. 2 and 3 are bi-linear functions of \mathbf{h} and we use a squared-error objective:

$$J = \frac{1}{2} \|r(\mathbf{y}|\mathbf{x}) - \mathbf{y}\|^2. \quad (4)$$

We can also constrain the GAE to be a symmetric model by training it to reconstruct both \mathbf{x} given \mathbf{y} and \mathbf{y} given \mathbf{x} (Memisevic, 2011):

$$J = \frac{1}{2} \|r(\mathbf{y}|\mathbf{x}) - \mathbf{y}\|^2 + \frac{1}{2} \|r(\mathbf{x}|\mathbf{y}) - \mathbf{x}\|^2. \quad (5)$$

The symmetric objective can be thought of as the non-probabilistic analogue of modeling a *joint* distribution over \mathbf{x} and \mathbf{y} as opposed to a conditional (Memisevic, 2011).

3 GATED AUTO-ENCODER SCORING

In (Kamyshanska & Memisevic, 2013), the authors showed that data could be scored under an auto-encoder by interpreting the model as a *dynamical system*. In contrast to the probabilistic views based

¹Relational features can be mixed with standard features by simply adding connections that are not gated.

on score matching (Swersky et al., 2011; Vincent, 2010; Guillaume & Bengio, 2013) and regularization, the dynamical systems approach permits scoring under models with either linear (real-valued data) or sigmoid (binary data) outputs, as well as arbitrary hidden unit activation functions. The method is also agnostic to the learning procedure used to train the model, meaning that it is suitable for the various types of regularized auto-encoders which have been proposed recently. In this section, we demonstrate how the dynamical systems view can be extended to the GAE.

3.1 VECTOR FIELD REPRESENTATION

Similar to (Kamyshanska & Memisevic, 2013), we will view the GAE as a dynamical system with the vector field defined by

$$F(\mathbf{y}|\mathbf{x}) = r(\mathbf{y}|\mathbf{x}) - \mathbf{y}.$$

The vector field represents the local transformation that $\mathbf{y}|\mathbf{x}$ undergoes as a result of applying the reconstruction function $r(\mathbf{y}|\mathbf{x})$. Repeatedly applying the reconstruction function to an input $\mathbf{y}|\mathbf{x} \rightarrow r(\mathbf{y}|\mathbf{x}) \rightarrow r(r(\mathbf{y}|\mathbf{x})|\mathbf{x}) \rightarrow \dots \rightarrow r(\dots r(\mathbf{y}|\mathbf{x})|\mathbf{x})$ yields a trajectory whose dynamics, from a physics perspective, can be viewed as a force field. At any point, the potential force acting on a point is the gradient of some potential energy (negative goodness) at that point. In this light, the GAE reconstruction may be viewed as pushing pairs of inputs \mathbf{x}, \mathbf{y} in the direction of lower energy.

Our goal is to derive the energy function, which we call a scoring function, and which measures how much a GAE “likes” a given pair of inputs (\mathbf{x}, \mathbf{y}) up to normalizing constant. In order to find an expression for the potential energy, the vector field must be able to be written as the derivative of a scalar field (Kamyshanska & Memisevic, 2013). To check this, we can submit to Poincaré’s integrability criterion: For some open, simple connected set \mathcal{U} , a continuously differentiable function $F : \mathcal{U} \rightarrow \mathbb{R}^m$ defines a gradient field if and only if

$$\frac{\partial F_i(\mathbf{y})}{\partial y_j} = \frac{\partial F_j(\mathbf{y})}{\partial y_i}, \forall i, j = 1 \dots n.$$

The vector field defined by the GAE indeed satisfies Poincaré’s integrability criterion; therefore it can be written as the derivative of a scalar field. A derivation is given in Appendix A.1. This also applies to the GAE with a symmetric objective function (Eq. 5) by setting the input as $\xi|\gamma$ such that $\xi = [\mathbf{y}; \mathbf{x}]$ and $\gamma = [\mathbf{x}; \mathbf{y}]$ and following the exact same procedure.

3.2 SCORING THE GAE

As mentioned in Section 3.1, our goal is to find an energy surface, so that we can express the energy for a specific pair (\mathbf{x}, \mathbf{y}) . From the previous section, we showed that Poincaré’s criterion is satisfied and this implies that we can write the vector field as the derivative of a scalar field. Moreover, it illustrates that this vector field is a conservative field and this means that the vector field is a gradient of some scalar function, which in this case is the energy function of a GAE:

$$r(\mathbf{y}|\mathbf{x}) - \mathbf{y} = \nabla E.$$

Hence, by integrating out the trajectory of the GAE (\mathbf{x}, \mathbf{y}) , we can measure the energy along a path. Moreover, the line integral of a conservative vector field is path independent, which allows us to take the anti-derivative of the scalar function:

$$\begin{aligned} E(\mathbf{y}|\mathbf{x}) &= \int (r(\mathbf{y}|\mathbf{x}) - \mathbf{y}) d\mathbf{y} = \int W^Y ((W^X \mathbf{x}) \odot W^H h(\mathbf{u})) d\mathbf{y} - \int \mathbf{y} d\mathbf{y} \\ &= W^Y \left((W^X \mathbf{x}) \odot W^H \int h(\mathbf{u}) d\mathbf{y} \right) - \int \mathbf{y} d\mathbf{y}, \end{aligned} \quad (6)$$

where \mathbf{u} is an auxiliary variable such that $\mathbf{u} = W^H((W^Y \mathbf{y}) \odot (W^X \mathbf{x}))$ and $\frac{d\mathbf{u}}{d\mathbf{y}} = W^H(W^Y \odot (W^X \mathbf{x} \otimes \mathbf{1}_D))$, and \otimes is the Kronecker product. Moreover, the decoder can be re-formulated as

$$\begin{aligned} r(\mathbf{y}|\mathbf{x}) &= (W^Y)^T (W^X \mathbf{x} \odot (W^H)^T h(\mathbf{y}, \mathbf{x})) \\ &= ((W^Y)^T \odot (W^X \mathbf{x} \otimes \mathbf{1}_D)) (W^H)^T h(\mathbf{y}, \mathbf{x}). \end{aligned}$$

Re-writing Eq. 6 in terms of the auxiliary variable \mathbf{u} , we get

$$\begin{aligned} E(\mathbf{y}|\mathbf{x}) &= ((W^Y)^T \odot (W^Y \mathbf{x} \otimes \mathbf{1}_D)) (W^H)^T \int h(\mathbf{u}) (W^H (W^Y \odot (W^X \mathbf{x} \otimes \mathbf{1}_D)))^{-1} d\mathbf{u} - \int \mathbf{y} d\mathbf{y} \\ &= \int h(\mathbf{u}) d\mathbf{u} - \frac{1}{2} \mathbf{y}^2 + \text{const.} \end{aligned} \quad (7)$$

A more detailed derivation from Eq. 6 to Eq. 7 is provided in Appendix A.2. Identical to (Kamyshanska & Memisevic, 2013), if $h(\mathbf{u})$ is an element-wise activation function and we know its anti-derivative, then it is very simple to compute $E(\mathbf{x}, \mathbf{y})$.

4 RELATIONSHIP TO RESTRICTED BOLTZMANN MACHINES

In this section, we relate GAEs through the scoring function to other types of Restricted Boltzmann Machines, such as the Factored Gated Conditional RBM (Taylor & Hinton, 2009) and the Mean-covariance RBM (Ranzato & Hinton, 2010).

4.1 GATED AUTO-ENCODER AND FACTORED GATED CONDITIONAL RESTRICTED BOLTZMANN MACHINES

Kamyshanska & Memisevic (2013) showed that several hidden activation functions defined gradient fields, including sigmoid, softmax, tanh, linear, rectified linear function (ReLU), modulus, and squaring. These activation functions are applicable to GAEs as well.

In the case of the sigmoid activation function, $\sigma = h(\mathbf{u}) = \frac{1}{1+\exp(-\mathbf{u})}$, our energy function becomes

$$\begin{aligned} E_\sigma &= 2 \int (1 + \exp(-\mathbf{u}))^{-1} d\mathbf{u} - \frac{1}{2} (\mathbf{x}^2 + \mathbf{y}^2) + \text{const}, \\ &= 2 \sum_k \log(1 + \exp(W_k^H (W_k^X \mathbf{x} \odot W_k^X \mathbf{y}))) - \frac{1}{2} (\mathbf{x}^2 + \mathbf{y}^2) + \text{const}. \end{aligned}$$

Note that if we consider the conditional GAE we reconstruct \mathbf{x} given \mathbf{y} only, this yields

$$E_\sigma(\mathbf{y}|\mathbf{x}) = \sum_k \log(1 + \exp(W_k^H (W_k^Y \mathbf{y} \odot W_k^X \mathbf{x}))) - \frac{\mathbf{y}^2}{2} + \text{const}. \quad (8)$$

This expression is identical, up to a constant, to the free energy in a Factored Gated Conditional Restricted Boltzmann Machine (FCRBM) with Gaussian visible units and Bernoulli hidden units. We have ignored biases for simplicity. A derivation including biases is shown in Appendix B.1.

4.2 MEAN-COVARIANCE AUTO-ENCODER AND MEAN-COVARIANCE RESTRICTED BOLTZMANN MACHINES

The Covariance auto-encoder (cAE) was introduced in (Memisevic, 2011). It is a specific form of symmetrically trained auto-encoder with identical inputs: $\mathbf{x} = \mathbf{y}$, and tied input weights: $W^X = W^Y$. It maintains a set of relational mapping units to model covariance between pixels. One can introduce a separate set of mapping units connected pairwise to only one of the inputs which model the mean intensity. In this case, the model becomes a Mean-covariance auto-encoder (mcAE).

Theorem 1. Consider a cAE with encoder and decoder:

$$\begin{aligned} h(\mathbf{x}) &= h(W^H ((W^X \mathbf{x})^2) + \mathbf{b}) \\ r(\mathbf{x}|h) &= (W^X)^T (W^X \mathbf{x} \odot (W^H)^T h(\mathbf{x})) + \mathbf{a}, \end{aligned}$$

where $\theta = \{W^X, W^H, \mathbf{a}, \mathbf{b}\}$ are the parameters of the model, and $h(\mathbf{z}) = \frac{1}{1+\exp(-\mathbf{z})}$ is a sigmoid. Moreover, consider a Covariance RBM (Ranzato & Hinton, 2010) with Gaussian-distributed visibles and Bernoulli-distributed hiddens, with an energy function defined by

$$E^c(\mathbf{x}, \mathbf{h}) = \frac{(\mathbf{a} - \mathbf{x})^2}{\sigma^2} - \sum_f \text{Ph}(C\mathbf{x})^2 - \mathbf{b}\mathbf{h}.$$

Then the energy function of the cAE with dynamics $r(\mathbf{x}|\mathbf{y}) - \mathbf{x}$ is equivalent to the free energy of Covariance RBM up to a constant:

$$E(\mathbf{x}, \mathbf{x}) = \sum_k \log(1 + \exp(W^H(W^X \mathbf{x})^2 + \mathbf{b})) - \frac{\mathbf{x}^2}{2} + \text{const.} \quad (9)$$

The proof is given in Appendix B.2. We can extend this analysis to the mcAE by using the above theorem and the results from (Kamyshanska & Memisevic, 2013).

Corollary 1.1. *The energy function of a mcAE and the free energy of a Mean-covariance RBM (mcRBM) with Gaussian-distributed visibles and Bernoulli-distributed hidden are equivalent up to a constant. The energy of the mcAE is:*

$$E = \sum_k \log(1 + \exp(-W^H(W^X \mathbf{x})^2 - \mathbf{b})) + \sum_k \log(1 + \exp(W \mathbf{x} + \mathbf{c})) - \mathbf{x}^2 + \text{const} \quad (10)$$

where $\theta^m = \{W, \mathbf{c}\}$ parameterizes the mean mapping units and $\theta^c = \{W^X, W^H, \mathbf{a}, \mathbf{b}\}$ parameterizes the covariance mapping units.

Proof. The proof is very simple. Let $E_{mc} = E_m + E_c$, where E_m is the energy of the mean auto-encoder, E_c is the energy of the covariance auto-encoder, and E_{mc} is the energy of the mcAE. We know from Theorem 1 that E_c is equivalent to the free energy of a covariance RBM, and the results from (Kamyshanska & Memisevic, 2013) show that E_m is equivalent to the free energy of mean (classical) RBM. As shown in (Ranzato & Hinton, 2010), the free energy of a mcRBM is equal to summing the free energies of a mean RBM and a covariance RBM. \square

5 CLASSIFICATION WITH GATED AUTO-ENCODERS

Kamyshanska & Memisevic (2013) demonstrated that one application of the ability to assign energy or scores to auto-encoders was in constructing a classifier from class-specific auto-encoders. In this section, we explore two different paradigms for classification. Similar to that work, we consider the usual multi-class problem by first training class-specific auto-encoders, and using their energy functions as confidence scores. We also consider the more challenging structured output problem, specifically, the case of multi-label prediction where a data point may have more than one associated label, and there may be correlations among the labels.

5.1 CLASSIFICATION USING CLASS-SPECIFIC GATED AUTO-ENCODERS

One approach to classification is to take several class-specific models and assemble them into a classifier. The best-known example of this approach to fit several directed graphical models and use Bayes' rule to combine them. The process is simple because the models are normalized, or calibrated. While it is possible to apply a similar technique to undirected or non-normalized models such as auto-encoders, one must take care to calibrate them.

The approach proposed in (Kamyshanska & Memisevic, 2013) is to train K class-specific auto-encoders, each of which assigns a non-normalized energy to the data $E_i(\mathbf{x})$, $i = 1 \dots, K$, and then define the conditional distribution over classes z_i as

$$P(z_i|\mathbf{x}) = \frac{\exp(E_i(\mathbf{x}) + B_i)}{\sum_j \exp(E_j(\mathbf{x}) + B_j)}, \quad (11)$$

where B_i is a learned bias for class i . The bias terms take the role of calibrating the unnormalized energies. Note that we can similarly combine the energies from a symmetric gated auto-encoder where $\mathbf{x} = \mathbf{y}$ (i.e. a covariance auto-encoder) and apply Eq. 11. If, for each class, we train both a covariance auto-encoder and a classical auto-encoder (i.e. a "mean" auto-encoder) then we can combine both sets of unnormalized energies as follows

$$P_{mcAE}(z_i|\mathbf{x}) = \frac{\exp(E_i^M(\mathbf{x}) + E_i^C(\mathbf{x}) + B_i)}{\sum_j \exp(E_j^M(\mathbf{x}) + E_j^C(\mathbf{x}) + B_j)}, \quad (12)$$

where $E_i^M(\mathbf{x})$ is the energy which comes from the “mean” (standard) auto-encoder trained on class i and $E_i^C(\mathbf{x})$ the energy which comes from the “covariance” (gated) auto-encoder trained on class i . We call the classifiers in Eq. 11 and Eq. 12 “Covariance Auto-encoder Scoring” (cAES) and “Mean-Covariance Auto-encoder Scoring” (mcAES), respectively.

The training procedure is summarized as follows:

1. Train a (mean)-covariance auto-encoder individually for each class. Both the mean and covariance auto-encoder have tied weights in the encoder and decoder. The covariance auto-encoder is a gated auto-encoder with tied inputs.
2. Learn the B_i calibration terms using maximum likelihood, and backpropagate to the GAE parameters.

5.1.1 EXPERIMENTAL RESULTS

We followed the same experimental setup as (Memisevic et al., 2010) where we used a standard set of “Deep Learning Benchmarks” (Larochelle et al., 2007). We used mini-batch stochastic gradient descent to optimize parameters during training. The hyper-parameters: number of hidden, number of factors, corruption level, learning rate, weight-decay, momentum rate, and batch sizes were chosen based on a held-out validation set. Corruption levels and weight-decay were selected from $\{0, 0.1, 0.2, 0.3, 0.4, 0.5\}$, and number of hidden and factors were selected from 100,300,500. We selected the learning rate and weight-decay from the range (0.001, 0.0001).

Classification error results are shown in Table 1. First, the error rates of auto-encoder scoring variant methods illustrate that across all datasets AES outperforms cAES and mcAES outperforms both AES and cAES. AE models pixel means and cAE models pixel covariance, while mcAE models both mean and covariance, making it naturally more expressive. We observe that cAES and mcAES achieve lower error rates by a large margin on rotated MNIST with backgrounds (final row). On the other hand, both cAES and mcAES perform poorly on MNIST with random white noise background (second row from bottom). We believe this phenomenon is due to the inability to model covariance in this dataset. In MNIST with random white noise the pixels are typically uncorrelated, where in rotated MNIST with backgrounds the correlations are present and consistent.

DATA	SVM	RBM	DEEP	GSM	AES	cAES	mcAES
	RBF		SAA ₃				
RECT	2.15	4.71	2.14	0.56	0.84	0.61	0.54
RECT _{IMG}	24.04	23.69	24.05	22.51	21.45	22.85	21.41
CONVEX	19.13	19.92	18.41	17.08	21.52	21.6	20.63
MNIST _{SMALL}	3.03	3.94	3.46	3.70	2.61	3.65	3.65
MNIST _{ROT}	11.11	14.69	10.30	11.75	11.25	16.5	13.42
MNIST _{RAND}	14.58	9.80	11.28	10.48	9.70	18.65	16.73
MNIST _{ROTIM}	55.18	52.21	51.93	55.16	47.14	39.98	35.52

Table 1: Classification error rates on the Deep Learning Benchmark dataset. SAA₃ stands for three-layer Stacked Auto-encoder. SVM and RBM results are from (Vincent, 2010), DEEP and GSM are results from (Memisevic, 2011), and AES is from (Kamyschanska & Memisevic, 2013).

5.2 MULTI-LABEL CLASSIFICATION VIA OPTIMIZATION IN LABEL SPACE

The dominant application of deep learning approaches to vision has been the assignment of images to discrete classes (e.g. object recognition). Many applications, however, involve “structured outputs” where the output variable is high-dimensional and has a complex, multi-modal joint distribution. Structured output prediction may include tasks such as multi-label classification where there are regularities to be learned in the output, and segmentation, where the output is as high-dimensional as the input. A key challenge to such approaches lies in developing models that are able to capture complex, high level structure like shape, while still remaining tractable.

Though our proposed work is based on a deterministic model, we have shown that the energy, or scoring function of the GAE is equivalent, up to a constant, to that of a conditional RBM, a model that has already seen some use in structured prediction problems (Mnih et al., 2011; Li et al., 2013).

GAE scoring can be applied to structured output problems as a type of “post-classification” (Mnih & Hinton, 2010). The idea is to let a naïve, non-structured classifier make an initial prediction of the outputs in a fast, feed-forward manner, and then allow a second model (in our case, a GAE) clean up the outputs of the first model. Since GAEs can model the relationship between input \mathbf{x} and structured output \mathbf{y} , we can initialize the output with the output of the naïve model, and then optimize its energy function with respect to the outputs. Input \mathbf{x} is held constant throughout the optimization.

Li et al. (2013) recently proposed Compositional High Order Pattern Potentials, a hybrid of Conditional Random Fields (CRF) and Restricted Boltzmann Machines. The RBM provides a global shape information prior to the locally-connected CRF. Adopting the idea of *learning* structured relationships between outputs, we propose an alternate approach which the inputs of the GAE are not (\mathbf{x}, \mathbf{y}) but (\mathbf{y}, \mathbf{y}) . In other words, the post-classification model is a covariance auto-encoder. The intuition behind the first approach is to use a GAE to learn the relationship between the input \mathbf{x} and the output \mathbf{y} , whereas the second method aims to learn the correlations between the outputs \mathbf{y} .

We denote our two proposed methods GAE_{XY} and GAE_{Y^2} . GAE_{XY} corresponds to a GAE, trained conditionally, whose mapping units directly model the relationship between input and output and GAE_{Y^2} corresponds to a GAE which models correlations between output dimensions. GAE_{XY} defines $E(\mathbf{y}|\mathbf{x})$, while GAE_{Y^2} defines $E(\mathbf{y}|\mathbf{y}) = E(\mathbf{y})$. They differ only in terms of the data vectors that they consume. The training and test procedures are detailed in Algorithm 1.

Algorithm 1 Structured Output Prediction with GAE scoring

- 1: **procedure** MULTI-LABEL CLASSIFICATION($\mathcal{D} = \{(\mathbf{x}_i, \mathbf{y}_i) \in \mathcal{X}_{train} \times \mathcal{Y}_{train}\}$)
- 2: Train a Multi-layer Perceptron (MLP) to learn an input-output mapping $f(\cdot)$:

$$\underset{\theta_1}{\operatorname{argmin}} l(\mathbf{x}, \mathbf{y}; \theta_1) = \sum_i \operatorname{loss}_1((f(\mathbf{x}_i; \theta_1) - \mathbf{y}_i) \quad (13)$$

where loss_1 is an appropriate loss function for the MLP.

- 3: Train a Gated Auto-encoder with inputs $(\mathbf{x}_i, \mathbf{y}_i)$; For the case of GAE_{Y^2} , set $\mathbf{x}_i = \mathbf{y}_i$.

$$\underset{\theta_2}{\operatorname{argmin}} l(\mathbf{x}, \mathbf{y}; \theta_2) = \sum_i \operatorname{loss}_2(r(\mathbf{y}_i|\mathbf{x}_i, \theta_2) - \mathbf{y}_i) \quad (14)$$

where loss_2 is an appropriate reconstructive loss for the auto-encoder.

- 4: **for** each test data point $\mathbf{x}_i \in \mathcal{X}_{test}$ **do**
- 5: Initialize the output using the MLP.

$$\mathbf{y}_0 = f(\mathbf{x}_{test}) \quad (15)$$

- 6: **while** $\|E(\mathbf{y}_{t+1}|\mathbf{x}) - E(\mathbf{y}_t|\mathbf{x})\| > \epsilon$ or $\leq \text{max. iter.}$ **do**
 - 7: Compute $\nabla_{\mathbf{y}_t} E$
 - 8: Update $\mathbf{y}_{t+1} = \mathbf{y}_t - \lambda \nabla_{\mathbf{y}_t} E$
 - 9: where ϵ is the tolerance rate with respect to the convergence of the optimization.
-

5.2.1 EXPERIMENTAL RESULTS

We consider multi-label classification, where the problem is to classify instances which can take on more than one label at a time. We followed the same experimental set up as (Mnih et al., 2011). Four multi-labeled datasets were considered: Yeast (Elisseeff & Weston, 2002) consists of biological attributes, Scene (Boutell et al., 2004) is image-based, and MTurk (Mandel et al., 2010) and MajMin (Mandel & Ellis, 2008) are targeted towards tagging music. Yeast consists of 103 biological attributes and has 14 possible labels, Scene consists of 294 image pixels with 6 possible labels, and MTurk and MajMin each consist of 389 audio features extracted from music and have 92 and 96 possible tags, respectively. Figure 1 visualizes the covariance matrix for the label dimensions in each dataset. We can see from this that there are correlations present in the labels which suggests that a structured approach may improve on a non-structured predictor.

We compared our proposed approaches to logistic regression, a standard MLP, and the two structured CRBM training algorithms presented in (Mnih et al., 2011). To permit a fair comparison, we followed the same procedure for training and reporting errors as in that paper, where we cross val-

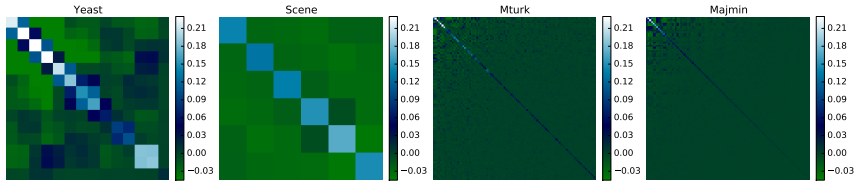


Figure 1: Covariance matrices for the multi-label datasets: Yeast, Scene, MTurk, and MajMin.

idated over 10 folds and training, validation, test examples are randomly separated into 80%, 10%, and 10% in each fold. The error rate was measured by averaging the errors on each label dimension.

Method	Yeast	Scene	MTurk	MajMin
LogReg	20.16	10.11	8.10	4.34
HashCRBM*	20.02	8.80	7.24	4.24
MLP	19.79	8.99	7.13	4.23
GAES _{XY}	19.27	6.83	6.59	3.96
GAES _{Y2}	19.58	6.81	6.59	4.29

Figure 2: Error rate on multi-label datasets. We report standard errors across 10 repeated runs with different random weight initializations. Note that LogReg and HashCRBM are taken from (Mnih et al., 2011) and we therefore do not report standard errors.

The performance on four multi-label datasets is shown in Table 2. We observed that adding a small amount of Gaussian noise to the input y improved the performance for GAE_{XY}. However, adding noise to the input x did not have as much of an effect. We suspect that adding noise makes the GAE more robust to the input provided by the MLP. Interestingly, we found that the performance of GAE_{Y2} was negatively affected by adding noise. Both of our proposed methods, GAES_{XY} and GAES_{Y2} generally outperformed the other methods except for GAES_{Y2} on the MajMin dataset. At least for these datasets, there is no clear winner between the two. GAES_{XY} achieved lower error than GAES_{Y2} for Yeast and MajMin, and the same error rate on the MTurk dataset. However, GAES_{Y2} outperforms GAES_{XY} on the Scene dataset. Overall, the results show that GAE scoring may be a promising means of post-classification in structured output prediction.

6 CONCLUSION

There have been many theoretical and empirical studies on auto-encoders (Vincent et al., 2008; Rifai, 2011; Swersky et al., 2011; Vincent, 2010; Guillaume & Bengio, 2013; Kamyshanska & Memisevic, 2013), however, the theoretical study of gated auto-encoders is limited apart from (Memisevic, 2011; Droniou & Sigaud, 2013). The GAE has several intriguing properties that a classical auto-encoder does not, based on its ability to model relations among pixel intensities rather than just the intensities themselves. This opens up a broader set of applications. In this paper, we derive some theoretical results for the GAE that enable us to gain more insight and understanding of its operation.

We cast the GAE as a dynamical system driven by a vector field in order to analyze the model. In the first part of the paper, by following the same procedure as (Kamyshanska & Memisevic, 2013), we showed that the GAE could be scored according to an energy function. From this perspective, we demonstrated the equivalency of the GAE energy to the free energy of a FCRBM with Gaussian visible units, Bernoulli hidden units, and sigmoid hidden activations. In the same manner, we also showed that the covariance auto-encoder can be formulated in a way such that its energy function is the same as the free energy of a covariance RBM, and this naturally led to a connection between the mean-covariance auto-encoder and mean-covariance RBM. One interesting observation is that Gaussian-Bernoulli RBMs have been reported to be difficult to train (Krizhevsky, 2009; Cho et al., 2011), and the success of training RBMs is highly dependent on the training setup (Wang et al., 2014). Auto-encoders are an attractive alternative, even when an energy function is required.

Structured output prediction is a natural next step for representation learning. The main advantage of our approach compared to other popular approaches such as Markov Random Fields, is that inference over is extremely fast, using a gradient-based optimization of the auto-encoder scoring function. In the future, we plan on tackling more challenging structured output prediction problems.

REFERENCES

- Bengio, Yoshua and Thibodeau-Laufer, Éric. Deep generative stochastic networks trainable by backprop. *arXiv preprint arXiv:1306.1091*, 2013.
- Boutell, Matthew R., Luob, Jiebo, Shen, Xipeng, and Brown, Christopher M. Learning multi-label scene classification. *Pattern Recognition*, 37:1757–1771, 2004.
- Cho, Kyunghyun, Ilin, Alexander, and Raiko, Tapani. Improved learning of gaussian-bernoulli restricted boltzmann machines. In *ICANN*, pp. 10–17, 2011.
- Droniou, Alain and Sigaud, Olivier. Gated autoencoders with tied input weights. In *ICML*, 2013.
- Elisseeff, Andre and Weston, Jason. A kernel method for multi-labelled classification. In *NIPS*, 2002.
- Guillaume, Alain and Bengio, Yoshua. What regularized auto-encoders learn from the data generating distribution. In *ICLR*, 2013.
- Kamyszanska, Hanna and Memisevic, Roland. On autoencoder scoring. In *ICML*, pp. 720–728, 2013.
- Krizhevsky, Alex. Learning multiple layers of features from tiny images. Technical report, Department of Computer Science, University of Toronto, 2009.
- Krizhevsky, Alex, Sutskever, Ilya, and Hinton, Geoffrey E. Imagenet classification with deep convolutional neural networks. In *NIPS*, 2012.
- Larochelle, Hugo, Erhan, Dumitru, Courville, Aaron, Bergstra, James, and Bengio, Yoshua. An empirical evaluation of deep architectures on problems with many factors of variation. In *ICML*, 2007.
- Li, Yujia, Tarlow, Daniel, and Zemel, Richard. Exploring compositional high order pattern potentials for structured output learning. In *CVPR*, 2013.
- Mandel, Michael I. and Ellis, Daniel P. W. A web-based game for collecting music metadata. *Journal New of Music Research*, 37:151–165, 2008.
- Mandel, Michael I., Eck, Douglas, and Bengio, Yoshua. Learning tags that vary within a song. In *ISMIR*, 2010.
- Memisevic, Roland. Gradient-based learning of higher-order image features. In *ICCV*, 2011.
- Memisevic, Roland, Zach, Christopher, Hinton, Geoffrey, and Pollefeys, Marc. Gated softmax classification. In *NIPS*, 2010.
- Mnih, Volodymyr and Hinton, Geoffrey. Learning to detect roads in high-resolution aerial images. In *Proceedings of the 11th European Conference on Computer Vision (ECCV)*, September 2010.
- Mnih, Volodymyr, Larochelle, Hugo, and Hinton, Geoffrey E. Conditional restricted boltzmann machines for structured output prediction. In *UAI*, 2011.
- Ranzato, MarcAurelio and Hinton, Geoffrey E. Modeling pixel means and covariances using factorized third-order boltzmann machines. In *CVPR*, 2010.
- Rifai, Salah. Contractive auto-encoders: Explicit invariance during feature extraction. In *ICML*, 2011.
- Swersky, K., Ranzato, MarcAurelio, Buchman, David, Freitas, Nando D., and Marlin, Benjamin M. On autoencoders and score matching for energy based models. In *ICML*, pp. 1201–1208, 2011.
- Szegedy, Christian, Liu, Wei, Jia, Yangqing, Sermanet, Pierre, Reed, Scott, Anguelov, Dragomir, Erhan, Dumitru, Vanhoucke, Vincent, and Rabinovich, Andrew. Going deeper with convolutions. *arXiv preprint arXiv:1409.4842*, 2014.
- Taylor, Graham W. and Hinton, Geoffrey E. Factored conditional restricted boltzmann machines for modeling motion style. In *ICML*, pp. 1025–1032, 2009.
- Vincent, Pascal. A connection between score matching and denoising auto-encoders. *Neural Computation*, 23(7):1661–1674, 2010.
- Vincent, Pascal, Larochelle, Hugo, Bengio, Yoshua, and Manzagol, P.A. Extracting and composing robust features with denoising autoencoders. In *ICML*, 2008.
- Wang, Nan, Melchior, Jan, and Wiskott, Laurenz. Gaussian-binary restricted boltzmann machines on modeling natural image statistics. Technical report, Institut für Neuroinformatik Ruhr-Universität Bochum, Bochum, 44780, Germany, 2014.

A GATED AUTO-ENCODER SCORING

A.1 VECTOR FIELD REPRESENTATION

To check that the vector field can be written as the derivative of a scalar field, we can submit to Poincaré's integrability criterion: For some open, simple connected set \mathcal{U} , a continuously differentiable function $F : \mathcal{U} \rightarrow \mathbb{R}^m$ defines a gradient field if and only if

$$\frac{\partial F_i(\mathbf{y})}{\partial y_j} = \frac{\partial F_j(\mathbf{y})}{\partial y_i}, \forall i, j = 1 \dots n.$$

Considering the GAE, note that i^{th} component of the decoder $r_i(\mathbf{y}|\mathbf{x})$ can be rewritten as

$$r_i(\mathbf{y}|\mathbf{x}) = (W_{\cdot i}^Y)^T (W^X \mathbf{x} \odot (W^H)^T h(\mathbf{y}, \mathbf{x})) = (W_{\cdot i}^Y \odot W^X \mathbf{x})^T (W^H)^T h(\mathbf{y}, \mathbf{x}).$$

The derivatives of $r_i(\mathbf{y}|\mathbf{x}) - y_i$ with respect to y_j are

$$\begin{aligned} \frac{\partial r_i(\mathbf{y}|\mathbf{x})}{\partial y_j} &= (W_{\cdot i}^Y \odot W^X \mathbf{x})^T (W^H)^T \frac{\partial h(\mathbf{x}, \mathbf{y})}{\partial y_j} = \frac{\partial r_j(\mathbf{y}|\mathbf{x})}{\partial y_i} \\ \frac{\partial h(\mathbf{y}, \mathbf{x})}{\partial y_j} &= \frac{\partial h(\mathbf{u})}{\partial \mathbf{u}} W^H (W_{\cdot j}^Y \odot W^X \mathbf{x}) \end{aligned} \quad (16)$$

where $\mathbf{u} = W^H((W^Y \mathbf{y}) \odot (W^X \mathbf{x}))$. By substituting Equation 16 into $\frac{\partial F_i}{\partial y_j}, \frac{\partial F_j}{\partial y_i}$, we have

$$\frac{\partial F_i}{\partial y_j} = \frac{\partial r_i(\mathbf{y}|\mathbf{x})}{\partial y_j} - \delta_{ij} = \frac{\partial r_j(\mathbf{y}|\mathbf{x})}{\partial y_i} - \delta_{ij} = \frac{\partial F_j}{\partial y_i}$$

where $\delta_{ij} = 1$ for $i = j$ and 0 for $i \neq j$. Similarly, the derivatives of $r_i(\mathbf{y}|\mathbf{x}) - y_i$ with respect to x_j are

$$\begin{aligned} \frac{\partial r_i(\mathbf{y}|\mathbf{x})}{\partial x_j} &= (W_{\cdot i}^Y \odot W_{\cdot j}^X)^T (W^H)^T h(\mathbf{x}, \mathbf{y}) + (W_{\cdot i}^Y \odot W^X \mathbf{x}) (W^H)^T \frac{\partial h}{\partial x_j} = \frac{\partial r_j(\mathbf{y}|\mathbf{x})}{\partial x_i}, \\ \frac{\partial h(\mathbf{y}, \mathbf{x})}{\partial x_j} &= \frac{\partial h(\mathbf{u})}{\partial \mathbf{u}} W^H (W_{\cdot j}^Y \odot W^X \mathbf{x}). \end{aligned} \quad (17)$$

By substituting Equation 17 into $\frac{\partial F_i}{\partial x_j}, \frac{\partial F_j}{\partial x_i}$, this yields

$$\frac{\partial F_i}{\partial x_j} = \frac{\partial r_i(\mathbf{x}|\mathbf{y})}{\partial x_j} = \frac{\partial r_j(\mathbf{x}|\mathbf{y})}{\partial x_i} = \frac{\partial F_j}{\partial x_i}.$$

A.2 DERIVING AN ENERGY FUNCTION

Integrating out the GAE's trajectory, we have

$$\begin{aligned} E(\mathbf{y}|\mathbf{x}) &= \int_{\mathcal{C}} (r(\mathbf{y}|\mathbf{x}) - \mathbf{y}) d\mathbf{y} \\ &= \int W^Y ((W^X \mathbf{x}) \odot W^H h(\mathbf{u})) d\mathbf{y} - \int \mathbf{y} d\mathbf{y} \\ &= W^Y \left((W^X \mathbf{x}) \odot W^H \int h(\mathbf{u}) d\mathbf{u} \right) - \int \mathbf{y} d\mathbf{y}, \end{aligned} \quad (18)$$

where \mathbf{u} is an auxiliary variable such that $\mathbf{u} = W^H((W^Y \mathbf{y}) \odot (W^X \mathbf{x}))$ and $\frac{d\mathbf{u}}{d\mathbf{y}} = W^H(W^Y \odot (W^X \mathbf{x} \otimes \mathbf{1}_D))$, where \otimes is the Kronecker product. Consider the symmetric objective function, which is defined in Equation 5. Then we have to also consider the vector field system where both symmetric cases $\mathbf{x}|\mathbf{y}$ and $\mathbf{y}|\mathbf{x}$ are valid. As mentioned in Section 3.1, let $\xi = [\mathbf{x}; \mathbf{y}]$ and $\gamma = [\mathbf{y}; \mathbf{x}]$. As well, let $W^\xi = \text{diag}(W^X, W^Y)$ and $W^\gamma = \text{diag}(W^Y, W^X)$ where they are block diagonal matrices. Consequently, the vector field becomes

$$F(\xi|\gamma) = r(\xi|\gamma) - \xi, \quad (19)$$

and the energy function becomes

$$\begin{aligned} E(\xi|\gamma) &= \int (r(\xi|\gamma) - \xi) d\xi \\ &= \int (W^\xi)^T ((W^\gamma \gamma) \odot (W^H)^T h(\mathbf{u})) d\xi - \int \xi d\xi \\ &= (W^\xi)^T ((W^\gamma \gamma) \odot (W^H)^T \int h(\mathbf{u}) d\mathbf{u}) - \int \xi d\xi \end{aligned}$$

where \mathbf{u} is an auxiliary variable such that $\mathbf{u} = W^H ((W^\xi \xi) \odot (W^\gamma \gamma))$. Then

$$\frac{d\mathbf{u}}{d\xi} = W^H (W^\xi \odot (W^\gamma \gamma \otimes \mathbf{1}_D)).$$

Moreover, note that the decoder can be re-formulated as

$$\begin{aligned} r(\xi|\gamma) &= (W^\xi)^T (W^\gamma \gamma \odot (W^H)^T h(\xi, \gamma)) \\ &= ((W^\xi)^T \odot (W^\gamma \gamma \otimes \mathbf{1}_D)) (W^H)^T h(\xi, \gamma). \end{aligned}$$

Re-writing the first term of Equation 18 in terms of the auxiliary variable \mathbf{u} , the energy reduces to

$$\begin{aligned} E(\xi|\gamma) &= ((W^\xi)^T \odot (W^\gamma \gamma \otimes \mathbf{1}_D)) (W^H)^T \int h(\mathbf{u}) (W^H (W^\xi \odot (W^\gamma \gamma \otimes \mathbf{1}_D)))^{-1} d\mathbf{u} - \int \xi d\xi \\ &= ((W^\xi)^T \odot (W^\gamma \gamma \otimes \mathbf{1}_D)) (W^H)^T ((W^\xi \odot (W^\gamma \gamma \otimes \mathbf{1}_D)) W^H)^{-T} \int h(\mathbf{u}) d\mathbf{u} - \int \xi d\xi \\ &= \int h(\mathbf{u}) d\mathbf{u} - \int \xi d\xi \\ &= \int h(\mathbf{u}) d\mathbf{u} - \frac{1}{2} \xi^2 + \text{const.} \end{aligned}$$

B RELATION TO OTHER TYPES OF RESTRICTED BOLTZMANN MACHINES

B.1 GATED AUTO-ENCODER AND FACTORED GATED CONDITIONAL RESTRICTED BOLTZMANN MACHINES

Suppose that the hidden activation function is a sigmoid. Moreover, we define our Gated Auto-encoder to consists of an encoder $h(\cdot)$ and decoder $r(\cdot)$ such that

$$\begin{aligned} h(\mathbf{x}, \mathbf{y}) &= h(W^H ((W^X \mathbf{x}) \odot (W^Y \mathbf{y})) + \mathbf{b}) \\ r(\mathbf{x}|\mathbf{y}, h) &= (W^X)^T ((W^Y \mathbf{y}) \odot (W^H)^T h(\mathbf{x}, \mathbf{y})) + \mathbf{a}, \end{aligned}$$

where $\theta = \{W^H, W^X, W^Y, \mathbf{b}\}$ is the parameters of the model. Note that the weights are not tied in this case. The energy function for the Gated Auto-encoder will be:

$$\begin{aligned} E_\sigma(\mathbf{x}|\mathbf{y}) &= \int (1 + \exp(-W^H (W^X \mathbf{x}) \odot (W^Y \mathbf{y}) - \mathbf{b}))^{-1} d\mathbf{u} - \frac{\mathbf{x}^2}{2} + \mathbf{a}\mathbf{x} + \text{const} \\ &= \sum_k \log(1 + \exp(-W_k^H (W^X \mathbf{x}) \odot (W^Y \mathbf{y}) - b_k)) - \frac{\mathbf{x}^2}{2} + \mathbf{a}\mathbf{x} + \text{const.} \end{aligned}$$

Now consider the free energy of a Factored Gated Conditional Restricted Boltzmann Machine (FCRBM).

The energy function of a FCRBM with Gaussian visible units and Bernoulli hidden units is defined by

$$E(\mathbf{x}, \mathbf{h}|\mathbf{y}) = \frac{(\mathbf{a} - \mathbf{x})^2}{2\sigma^2} - \mathbf{b}\mathbf{h} - \sum_f W_f^X \mathbf{x} \odot W_f^Y \mathbf{y} \odot W_f^H \mathbf{h}.$$

Given \mathbf{y} , the conditional probability density assigned by the FCRBM to data point \mathbf{x} is

$$p(\mathbf{x}|\mathbf{y}) = \frac{\sum_{\mathbf{h}} \exp(-E(\mathbf{x}, \mathbf{h}|\mathbf{y}))}{Z(\mathbf{y})} = \frac{\exp(-F(\mathbf{x}|\mathbf{y}))}{Z(\mathbf{y})}$$

$$-F(\mathbf{x}|\mathbf{y}) = \log \left(\sum_{\mathbf{h}} \exp(-E(\mathbf{x}, \mathbf{h}|\mathbf{y})) \right)$$

where $Z(\mathbf{y}) = \sum_{\mathbf{x}, \mathbf{h}} \exp(E(\mathbf{x}, \mathbf{h}|\mathbf{y}))$ is the partition function and $F(\mathbf{x}|\mathbf{y})$ is the free energy function. Expanding the free energy function, we get

$$\begin{aligned} -F(\mathbf{x}|\mathbf{y}) &= \log \sum_{\mathbf{h}} \exp(-E(\mathbf{x}, \mathbf{h}|\mathbf{y})) \\ &= \log \sum_{\mathbf{h}} \exp \left(-\frac{(\mathbf{a} - \mathbf{x})^2}{2\sigma^2} + \mathbf{b}\mathbf{h} + \sum_f W_f^X \mathbf{x} \odot W_f^Y \mathbf{y} \odot W_f^H \mathbf{h} \right) \\ &= -\frac{(\mathbf{a} - \mathbf{x})^2}{2\sigma^2} + \log \left(\sum_{\mathbf{h}} \exp \left(\mathbf{b}\mathbf{h} + \sum_f W_f^X \mathbf{x} \odot W_f^Y \mathbf{y} \odot W_f^H \mathbf{h} \right) \right) \\ &= -\frac{(\mathbf{a} - \mathbf{x})^2}{2\sigma^2} + \log \left(\sum_{\mathbf{h}} \prod_k \exp \left(b_k h_k + \sum_f (W_f^X \mathbf{x} \odot W_f^Y \mathbf{y}) \odot W_{fk}^H h_k \right) \right) \\ &= -\frac{(\mathbf{a} - \mathbf{x})^2}{2\sigma^2} + \sum_k \log \left(1 + \exp \left(b_k + \sum_f ((W_{fk}^H)^T (W_f^X \mathbf{x} \odot W_f^Y \mathbf{y})) \right) \right). \end{aligned}$$

Note that we can center the data by subtracting mean of \mathbf{x} and dividing by its standard deviation, and therefore assume that $\sigma^2 = 1$. Substituting, we have

$$\begin{aligned} -F(\mathbf{x}|\mathbf{y}) &= -\frac{(\mathbf{a} - \mathbf{x})^2}{2} + \sum_k \log \left(1 + \exp \left(-b_k - \sum_f (W_{fk}^H)^T (W_f^X \mathbf{x} \odot W_f^Y \mathbf{y}) \right) \right) \\ &= \sum_k \log \left(1 + \exp \left(b_k + \sum_f (W_{fk}^H)^T (W_f^X \mathbf{x} \odot W_f^Y \mathbf{y}) \right) \right) - \mathbf{a}^2 + \mathbf{a}\mathbf{x} - \frac{\mathbf{x}^2}{2} \\ &= \sum_k \log \left(1 + \exp \left(b_k + \sum_f (W_{fk}^H)^T (W_f^X \mathbf{x} \odot W_f^Y \mathbf{y}) \right) \right) + \mathbf{a}\mathbf{x} - \frac{\mathbf{x}^2}{2} + \text{const} \end{aligned}$$

Letting $W^H = (W^H)^T$, we get

$$= \sum_k \log \left(1 + \exp \left(b_k + \sum_f W_{kf}^H (W_f^X \mathbf{x} \odot W_f^Y \mathbf{y}) \right) \right) + \mathbf{a}\mathbf{x} - \frac{\mathbf{x}^2}{2} + \text{const}$$

Hence, the Conditional Gated Auto-encoder and the FCRBM are equal up to a constant.

B.2 GATED AUTO-ENCODER AND MEAN-COVARIANCE RESTRICTED BOLTZMANN MACHINES

Theorem 2. Consider a covariance auto-encoder with an encoder and decoder,

$$\begin{aligned} h(\mathbf{x}, \mathbf{x}) &= h(W^H((W^F \mathbf{x})^2) + \mathbf{b}) \\ r(\mathbf{x}|\mathbf{y} = \mathbf{x}, h) &= (W^F)^T (W^F \mathbf{y} \odot (W^H)^T h(\mathbf{x}, \mathbf{y})) + \mathbf{a}, \end{aligned}$$

where $\theta = \{W^F, W^H, \mathbf{a}, \mathbf{b}\}$ are the parameters of the model. Moreover, consider a covariance Restricted Boltzmann Machine with Gaussian distribution over the visibles and Bernoulli distribution

over the hiddens, such that its energy function is defined by

$$E^c(\mathbf{x}, \mathbf{h}) = \frac{(\mathbf{a} - \mathbf{x})^2}{\sigma^2} - \sum_f P\mathbf{h}(C\mathbf{x})^2 - \mathbf{b}\mathbf{h},$$

where $\theta = \{P, C, \mathbf{a}, \mathbf{b}\}$ are its parameters. Then the energy function for a covariance Auto-encoder with dynamics $r(\mathbf{x}|\mathbf{y}) - \mathbf{x}$ is equivalent to the free energy of a covariance Restricted Boltzmann Machine. The energy function of the covariance Auto-encoder is

$$E(\mathbf{x}, \mathbf{x}) = \sum_k \log(1 + \exp(W^H(W^F\mathbf{x})^2 + \mathbf{b})) - \mathbf{x}^2 + \text{const} \quad (20)$$

Proof. Note that the covariance auto-encoder is the same as a regular Gated Auto-encoder, but setting $\mathbf{y} = \mathbf{x}$ and making the factor loading matrices the same, i.e. $W^F = W^Y = W^X$. Then applying the general energy equation for GAE, Equation 7, to the covariance auto-encoder, we get

$$\begin{aligned} E(\mathbf{x}, \mathbf{x}) &= \int h(\mathbf{u})d\mathbf{u} - \frac{1}{2}\mathbf{x}^2 + \text{const} \\ &= \sum_k \log(1 + \exp(W^H(W^F\mathbf{x})^2 + \mathbf{b})) - \mathbf{x}^2 + \mathbf{a}\mathbf{x} + \text{const}, \end{aligned} \quad (21)$$

where $\mathbf{u} = W^H(W^F\mathbf{x})^2 + \mathbf{b}$.

Now consider the free energy of the mean-covariance Restricted Boltzmann Machine (mcRBM) with Gaussian distribution over the visible units and Bernoulli distribution over the hidden units:

$$\begin{aligned} -F(\mathbf{x}|\mathbf{y}) &= \log \sum_{\mathbf{h}} \exp(-E(\mathbf{x}, \mathbf{h}|\mathbf{y})) \\ &= \log \sum_h \exp\left(-\frac{(\mathbf{a} - \mathbf{x})^2}{\sigma^2} + (P\mathbf{h})(C\mathbf{x})^2 + \mathbf{b}\mathbf{h}\right) \\ &= \log \sum_h \prod_k \exp\left(-\frac{(\mathbf{a} - \mathbf{x})^2}{\sigma^2} + \sum_f (P_{fk}h_k)(C\mathbf{x})^2 + b_k h_k\right) \\ &= \sum_k \log \left(1 + \exp\left(\sum_f (P_{fk}h_k)(C\mathbf{x})^2\right)\right) - \frac{(\mathbf{a} - \mathbf{x})^2}{\sigma^2}. \end{aligned}$$

As before, we can center the data by subtracting mean of \mathbf{x} and dividing by its standard deviation, and therefore assume that $\sigma^2 = 1$. Substituting, we have

$$= \sum_k \log \left(1 + \exp\left(\sum_f (P_{fk}h_k)(C\mathbf{x})^2\right)\right) - (\mathbf{a} - \mathbf{x})^2. \quad (22)$$

Letting $W^H = P^T$ and $W^F = C$, we get

$$= \sum_k \log \left(1 + \exp\left(\sum_f (P_{fk}h_k)(C\mathbf{x})^2\right)\right) - \mathbf{x}^2 + \mathbf{a}\mathbf{x} + \text{const}. \quad (23)$$

Therefore, the two equations are equivalent. \square